

1 Article

2 **Characterization of overtopping waves on sea dikes** 3 **in gentle and shallow foreshores**

4 **Tomohiro Suzuki**^{1,2,*}, **Corrado Altomare**^{3,4}, **Tomohiro Yasuda**⁵ and **Toon Verwaest**¹

5 ¹ Flanders Hydraulics Research, 2140 Antwerp, Belgium; tomohiro.suzuki@mow.vlaanderen.be

6 ² Faculty of Civil Engineering and Geosciences, Delft University of Technology, 2628 CN Delft, The
7 Netherlands

8 ³ Maritime Engineering Laboratory, Department of Civil and Environmental Engineering, Universitat
9 Politècnica de Catalunya—BarcelonaTech (UPC), 08034 Barcelona, Spain, corrado.altomare@upc.edu

10 ⁴ Ghent University, Department of Civil Engineering, Technologiepark 60, 9052 Gent, Belgium

11 ⁵ Kansai University, tomo@oceanwave.jp

12 * Correspondence: tomohiro.suzuki@mow.vlaanderen.be; Tel.: +32-3-224-69-34

13 Received: date; Accepted: date; Published: date

14 **Abstract:** Due to the ongoing climate change, the overtopping risk is increasing. In order to have an
15 effective countermeasures, it is useful to understand overtopping processes in details. In this study
16 overtopping flow on a dike in gentle and shallow foreshores are investigated using SWASH. The
17 SWASH model in 2DV (i.e. flume like configuration) is first validated using the data of long crested
18 wave cases with second order wave generation in the physical model test conducted. After that it is
19 used to produce overtopping flow in different wave conditions and bathymetries. The results
20 indicated that the overtopping risk is better characterized by the time dependent h (overtopping
21 flow depth) and u (overtopping flow velocity) instead of h_{\max} (maximum overtopping flow depth)
22 and u_{\max} (maximum overtopping flow depth) and which will lead overestimation of the risk. The
23 time dependent u and h are strongly influenced by the dike configuration, namely by the
24 promenade width and the existence of the vertical wall on the promenade: the simulation shows
25 that the vertical wall induces seaward velocity on the dike which might be an extra risk during
26 extreme events.

27 **Keywords:** wave overtopping; average overtopping discharge; individual volume; overtopping
28 flow depth, overtopping flow velocity; promenade; vertical wall; SWASH

30 1. Introduction

31 The global climate change has manifold impacts on the ocean and its behaviour which directly
32 translates to the coastal/nearshore region as well as the governing processes. One such climate-
33 induced response is the increased frequency and intensity of extreme waves, leading to increased
34 overtopping risk for people living in coastal area [1,2]. One of the wave overtopping risks for people
35 is direct wave action which is not only relevant to pedestrians [3,4] and vehicles on a dike/promenade
36 but also to people in front of and inside dwellings and commercial buildings (e.g. hotels and
37 restaurants on dikes). There are some literature related to the stability of people on the
38 dikes/promenade [e.g. 3–5], which deal with the relationship between the human's stability and the
39 flow parameters (i.e. overtopping flow depth and flow velocity). Altomare et al. [6] also indicated
40 that the combination of overtopping flow velocity and flow depth rather than single maximum values
41 of one of these parameters is required to understand pedestrians hazard. Arrighi et al. [7,8] conducted
42 a numerical study on the human's stability and indicated that the relative submergence and Froude
43 number is a key. Other works focus on the characterization of overtopping flow depths and/or
44 velocities, see [9–12]. These are important works to understand the basic risk exposed to the flows on
45 dikes, however the present knowledge cannot cover all the risks due to different layouts and

46 hydraulic conditions. In a reality, often there are structures on the dike and thus the overtopping flow
47 characteristics are a bit more complex than the simplified assumptions (e.g. only plain promenade)
48 found in the literature. Overtopping flow can be changed by the interaction with structures. When
49 overtopping is severe, overtopping waves can destroy the facade (i.e. the first defense of the
50 dwellings/apartment buildings, such as windows and masonry walls, see examples in [13]), waves
51 can propagate further even inside buildings. Then the wave will be reflected to the seaward. The
52 return flow or reflected wave in front of a vertical wall can also influence the human's stability,
53 however a detailed discussion on such different flow directions has not been made explicitly so far.

54 As such, there are some knowledge gaps in the investigation on the risk of wave overtopping
55 flow on and behind sea dikes together with structures, and therefore it is important to discuss further
56 which physical process is relevant for the risk on people in the coastal area. As of today, the safety of
57 pedestrians and vehicles on coastal zones are often evaluated based on average overtopping
58 discharge, maximum individual volume and associated wave height in Eurotop [14]. For instance,
59 Eurotop indicates that individual overtopping volume V_{max} of 600 l/m in combination with $H_{m0}=1-3$
60 m is a limits for overtopping for people standing at seawall / dike crest with clear view of the sea but
61 it does not give further detailed explanation. Those are important indications but still it is not very
62 clear the applicability e.g. to the gentle and shallow foreshore cases [15]. Moreover, it is of interest
63 how a fixed criterion (e.g. 1 l/s/m or 10 l/s/m) can be linked to the overtopping characteristics such as
64 V_{max} (maximum individual volume), and time dependent h (overtopping flow depth) and u
65 (overtopping flow velocity). As Altomare et al. [6] indicated, the combination of u and h is linked to
66 the hazard rather than the single maximum values of one of these parameters. According to Suzuki
67 et al [16], gentle and very shallow foreshore will result in flatter spectrum at the toe of the dike and
68 thus spectral wave period is much longer than ones in deep water conditions [17]. In such a situation,
69 the waves have been transformed into bores and therefore overtopping characteristics, namely, flow
70 pattern on dikes /promenades, might be also different from one which toe is at deep water. However,
71 not so many studies have been conducted on the flow characteristics on dikes under gentle and
72 shallow foreshores and discussed the associated risk.

73 The purpose of this study is to investigate the relationship between q and other overtopping
74 parameters (V_{max} , h_{max} , u_{max} , V , h , u) on the dike with and without a vertical structure (i.e. a sea wall
75 or a building) in gentle and shallow foreshore, and eventually discuss the proper assessment method
76 for overtopping waves. To this end SWASH [18] is employed in this study. The model has been
77 validated for the case of wave overtopping over the impermeable dikes on gentle and shallow
78 foreshore configuration [16]. To ensure the applicability of the model to this study, relevant physical
79 model test data from CREST experiments is used for further validation. Using the validated model,
80 flow characteristics on a wide range of different hydraulic and topographic conditions are further
81 investigated. Note that SWASH can provide not only time dependent wave surface elevation but also
82 velocity field. By post-processing it is possible to calculate individual overtopping volumes and
83 average overtopping discharge too. Obtaining such outputs, especially the velocity fields on the dike,
84 is not an easy task in physical models since the velocity measurement points are exposed to wet and
85 dry conditions (when overtopping happens the bottom become wet while other moments are in
86 general dry) which often is a problem for velocimeters and thus numerical simulation is a good
87 alternative to study overtopping hazard.

88 2. Methods

89 2.1. SWASH

90 SWASH is based on Non-Linear Shallow Water equation with non-hydrostatic pressure terms.
91 The model can be run either in depth averaged mode or multi-layer mode. It is possible to maintain
92 frequency dispersion by increasing the number of layers. A model with two or three layers already
93 provides enough accuracy in terms of the frequency dispersion for most of the coastal applications.
94 Combining with HFA (hydrostatic front approximation [19]) the model can deal with wave breaking
95 with enough accuracy even in such a limited number of vertical layers. On top, non-linear wave
96 properties under breaking waves (e.g. asymmetry and skewness) are preserved. See more details in

97 [18]. Note that the use of SWASH is increasing as can be seen in the literature for the wide
98 applications, not limited to mere wave calculation but also for example interaction with ships [20],
99 interaction with vegetation [21] and wave interaction with rubble mound structures.

100 The features that SWASH offers, namely maintaining a good accuracy of wave transformation
101 and overtopping and is computationally not too demanding, are important factors for this study since
102 the model needs to capture the overtopping process on the sea-dike and at the same time it is
103 necessary to repeat calculations with different bathymetries, different water levels and wave
104 conditions. SWASH is computationally less demanding and thus it is easy to run a long duration (i.e.
105 1000 waves) and a large number of calculations. One drawback of SWASH model is that it cannot
106 deal with a complex structure such as a parapet. In such occasion, detailed wave modelling using
107 RANS models [22] or SPH models [23,24] can be an alternative however it is recommended to conduct
108 it in combination with light wave transformation models (e.g. [25,26]), otherwise it becomes
109 computationally very demanding to test different configurations.

110 2.2. Model settings

111 All the simulations are conducted in 2DV (two dimensional vertical). The version of the model
112 applied in this study is version 5.0. The grid size in the horizontal direction is 0.5 m in the prototype
113 scale as recommended in [27] which ensures a good wave propagation and overtopping processes.
114 The threshold water level (DEPMIN) is set 0.001 m for the prototype calculation, which increases the
115 computational stability compared to the default value. Two layers of equidistant layer distribution is
116 employed in this simulation in order to maintain good frequency dispersion and accuracy of second
117 order wave generation [28] so-called infragravity waves, which plays an important role for wave run-
118 up and overtopping process. Note that it is still possible to use one layer in terms of liner dispersion
119 since kh value of the test is less than 2.9 as indicated in the user manual however two layers are better
120 for the accuracy of the wave generation and propagation. Internal wave generation [29] has not been
121 used in this study since the reflection from the structure is very limited in this case.

122 As for the numeric, the Keller-box scheme is used for the simulation since the number of the
123 vertical layer is two. ILU preconditioner is employed for the computational robustness.

124 The momentum scheme is moment conservative. The standard first order up-wind scheme is
125 used for the discretization of the vertical term for w -momentum equation for the sake of stability of
126 the computation, while other discretization (i.e. the horizontal and vertical terms for u -momentum
127 equation and the horizontal term for w -momentum equation) used MUSCL limiter to achieve second
128 order accuracy. Time integration is explicit and a maximum Courant number of 0.5 is used to cope
129 with high and nonlinear waves used in this study.

130 The Manning formula with a Manning coefficient of 0.019 is employed to represent bottom
131 friction for the entire domain, both for sandy beach and the dike. Note that 0.019 is the recommended
132 value for wave simulations in the user manual. This must be due to the fact that the Manning's
133 coefficient for sand (e.g. the grain size of 0.3-0.4 mm) is around this value. For the dike it is assumed
134 that the bottom of the promenade is often like unfinished concrete, and which Manning's coefficient
135 is around 0.014-0.020 and thus 0.019 should be an acceptable choice. Standard wave breaking control
136 parameters, $\alpha=0.6$ and $\beta=0.3$ are used for wave breaking, and those values are also used in
137 [16].

138 2.3. Test matrix

139 As stated earlier, the purpose of the numerical experiment in this study is to obtain a wide range
140 variation of the overtopping in order to understand the overall overtopping flow characteristics on
141 the dike and in front of / inside buildings. Therefore the test matrix is designed to be able to obtain 4
142 different order of magnitude of wave overtopping discharges, namely 0.1, 1, 10, and 100 l/s/m. The
143 wide range of average overtopping discharges are achieved by changing the input hydraulic
144 conditions (i.e. water levels, offshore significant wave height) and bathymetries (i.e. toe level, dike
145 crest level, promenade width). The results will be further processed to discuss which physical
146 parameter is relevant to the risk of people at the coast. In total 96 cases for each configuration (Q and

147 W) of the numerical experiment have been conducted. For all the numerical experiment, a fixed seed
 148 number is used and the number of waves is 1000.

149 Table 1 shows the test matrix. The case name is specified according to the input conditions, e.g.
 150 RSK_Q_7_3_12_65_85_00. See next section for the detailed setting of the bathymetry.

151 **Table 1.** Variation of test parameters and the values

Name [-]	Bathymetry [-]	Water level [m]	H _{m0} [m]	T _p [m]	Toe level [m]	Dike crest level [m]	Promenade length [m]
RSK	Q	22 (7) ¹	3	12	21.5 (6.5) ¹	23.5 (8.5) ¹	0
		23 (8) ¹	4		21.9 (6.9) ¹	24.0 (9.0) ¹	20
	W		5			24.5 (9.5) ¹	
							25.0 (10.0) ¹

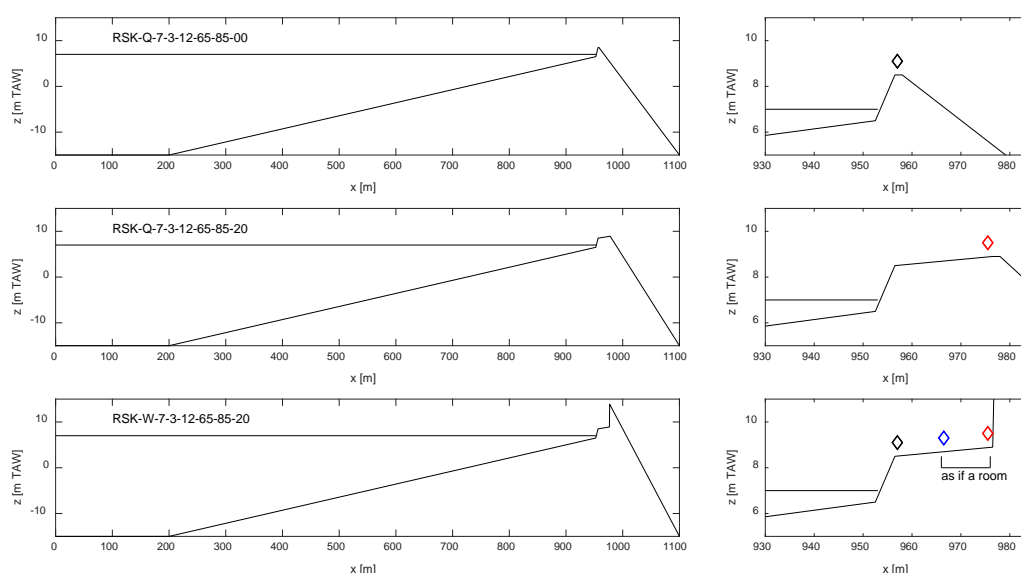
152 ¹ The value inside the brackets is based on [m TAW] (Tweede Algemene Waterpassing; Belgian standard
 153 datum level, situated near MLLWS) and the value is reflected in the case name.

154 **2.4. Bathymetry**

155 The level of the flat bottom in front of the wave generator is 0 m (-15 m TAW) and the length is
 156 200 m: it is slightly longer than one offshore wave length. The foreshore slope is fixed at 1/35 up to
 157 the dike toe at 21.5 and 21.9 m (6.5 and 6.9 m TAW). The slope of the dike is 1/2 and the promenade
 158 is 1/50. This is the base bathymetry which is applicable to both configurations (i.e. bathymetry Q and
 159 W).

160 Tests with bathymetry Q is aimed to obtain flow and overtopping properties (i.e. h, u, V, q) at
 161 the end of the promenade for both 0 m and 20 m, and thus no vertical wall at the end of them. Tests
 162 with bathymetry W is aimed to obtain overtopping flow properties (i.e. h, u) in front of a vertical wall
 163 on the promenade. This setting of W represents a situation of a promenade with a building, and at
 164 the same time inside a room under the assumption that the façade of the building does not exist. It is
 165 assumed a situation that the façade is already broken (and the ceiling is not reached).

166 Figure 1 shows the sketch of each bathymetry Q and W with different promenade width. The
 167 diamond points indicate the measurement points of flow and overtopping properties.



168 **Figure 1.** Bathymetries (type Q and W) and measurement points (black points: beginning, blue
 169 point: middle, red points: end of the promenade).

170 **2.5. Post-processing**

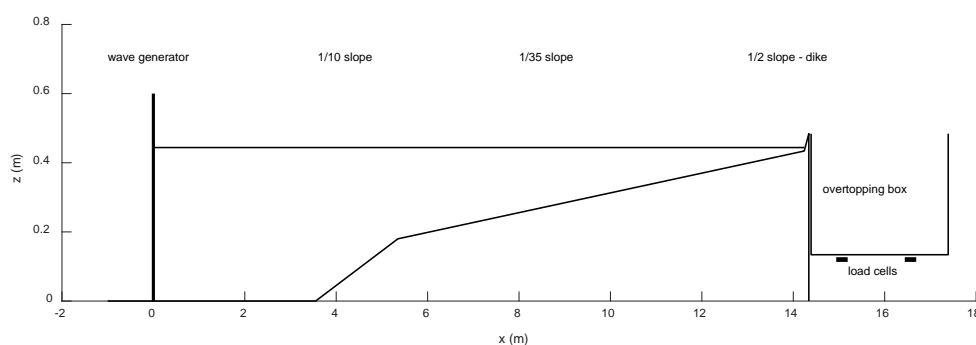
171 In SWASH, two equidistant layers are used for this simulation and the flow parameter u to be
 172 used in this study is the averaged value of the two velocities of the two layers.

173 In order to calculate the individual overtopping volume, water level criteria of 0.01 m is applied
 174 as a threshold. When the overtopping flow depth does not exceeds this value, the overtopping is not
 175 counted as one overtopping event.

176 V , h and u are the time dependent parameters, however, in order to discuss overtopping hazard,
 177 maximum values during 1000 waves' test are used and they are expressed as V_{\max} , h_{\max} and u_{\max} ,
 178 respectively. The values are the maximum ones, so it is sensitive to the exceedance probability: when
 179 a lower number of waves are applied, the maximum value will be lower.

180 2.5. Physical model

181 To validate the numerical model, data from a physical model test campaign conducted in
 182 Belgium (Climate Resilient Coast (CREST) project, <http://www.crestproject.be/>; see also details in
 183 [30]) is used. All the relevant data set to this study is the average overtopping discharge and
 184 individual volume measured at the end of dike slope (i.e. only promenade width 0 m). Since the
 185 SWASH model to be used in this study is run in 2DV (i.e. flume like configuration) based on the
 186 second order wave generation, only cases with long crested waves and second order generation in
 187 the 3D wave basin physical model are used for the validation. The bottom configuration of the
 188 physical model is not exactly the same as one in numerical model (Figure 2), however the main
 189 features of the physical model test such as the water depth and the main bottom slope and the dike
 190 slope are the same as this numerical experiment. The numerical experiment has a wide range of
 191 different configurations (i.e. toe level $\times 2$; dike crest level $\times 4$, and promenade length $\times 2$) and it
 192 includes the case of physical model (toe 6.5 m TAW, and dike crest 9.0 m TAW, promenade 0 m).



193 **Figure 2.** Cross section of foreshore and dike profile [30] in the 3D wave basin test.

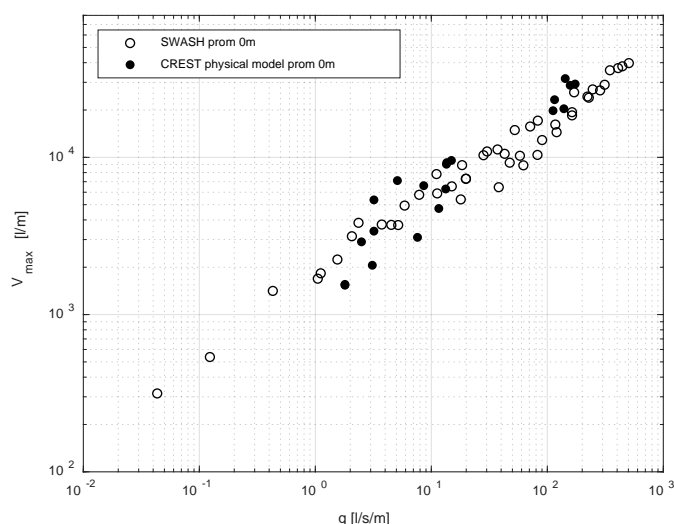
194

195 3. Results

196 3.1. Validation

197 The physical model test result of the maximum individual overtopping volume V_{\max} (data only
 198 limited to long crested and second order wave generation cases) is further processed and linked to
 199 the average overtopping discharge, see Figure 3. See [31] for further details of the data processing.

200 As can be seen in the figure the maximum individual overtopping volumes estimated by
 201 SWASH are in line with the physical model data. As shown in [32], SWASH can represent not only
 202 mean overtopping discharge over the dikes, but also wave run-up processes such as overtopping
 203 flow depth and velocity on the promenade, and wave force acting on a vertical wall on a dike.
 204 Therefore it can be concluded that the SWASH model is enough accurate and thus it is possible to
 205 explore further the wave overtopping characteristics on a dike in gentle and shallow foreshores based
 206 on the model.



207 **Figure 3.** Comparison between SWASH and physical model on q-Vmax (Average overtopping
 208 discharge - maximum individual overtopping volume) for the case of promenade width 0 m

209 3.2. Overtopping flow characteristics on a promenade (without a vertical wall)

210 In this section, overtopping flow properties on a promenade is investigated by SWASH. The
 211 used bathymetry is type Q, and thus there is no wall at the end of the promenade. This numerical
 212 experiment gives insights how overtopping flow properties which are not disturbed by a vertical
 213 wall behaves on the slightly sloped promenade.

214 3.2.1. q - V_{max} relationship

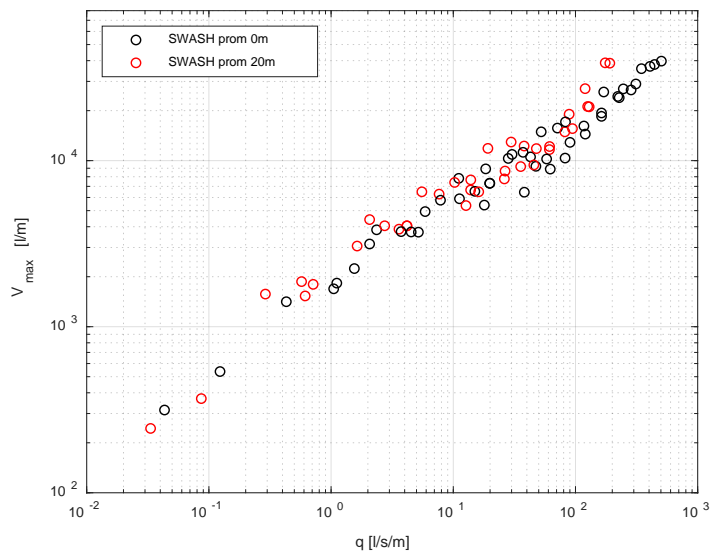
215 The relationship between q and V_{max} (maximum individual volume) for the cases with
 216 promenade length 0 and 20 m is shown in Figure 4.

217 As shown in the figure, 1 l/s/m gives maximum individual volume V_{max} around 2000 l/m, and 10
 218 l/s/m gives V_{max} around 6000 l/m for both promenade's cases: there is no significant differences
 219 between the two promenade widths. From this result it can be concluded that V_{max} is determined by
 220 q in the gentle and shallow foreshore case and the promenade width does not make significant
 221 difference on q- V_{max} relationship for the wide range of the input hydraulic conditions and
 222 bathymetries. Even though Alsop et al. (2008) indicated that the maximum individual overtopping
 223 volumes are more suitable hazard indicators, yet in this case V_{max} and q both give the same
 224 information. This might be due to the fact that the incident significant wave height in this shallow
 225 foreshore case is not significantly different at the toe of the dike (toe depth is 0.5 m) for different
 226 offshore wave conditions: wave height is limited by the shallow water depth.

227 3.2.2. q - h_{max} and q - u_{max} relationships

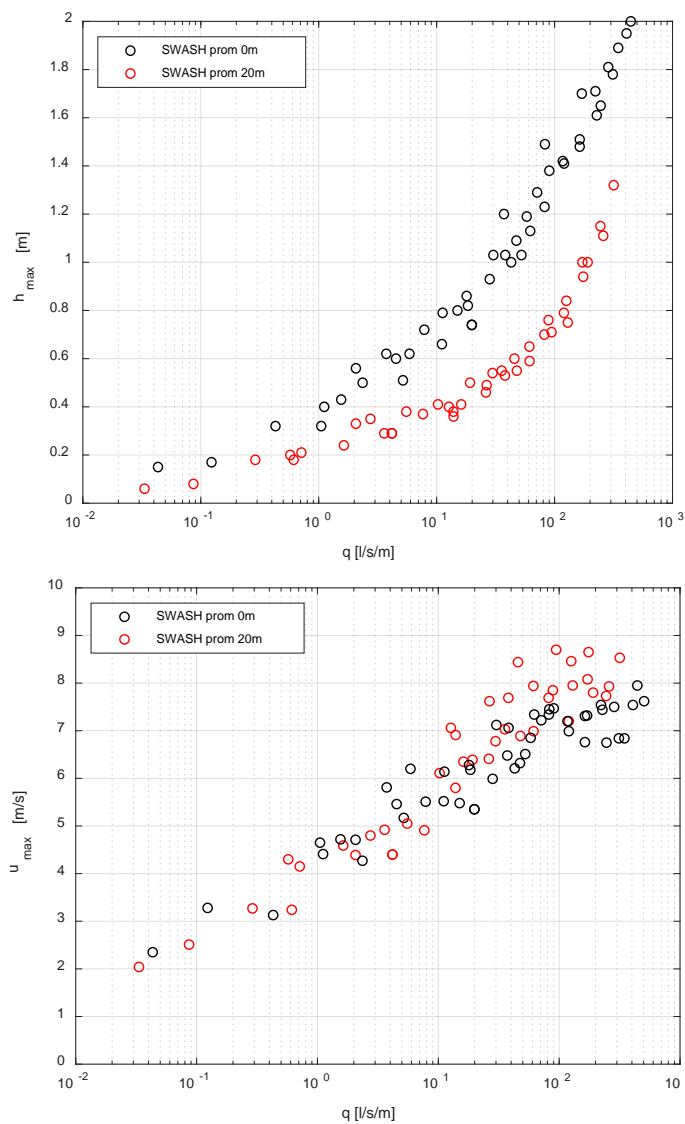
228 Next, the relationship q - h_{max} (maximum overtopping flow depth) and q - u_{max} (maximum
 229 overtopping flow velocity) for the cases with promenade length 0 and 20 m are shown in Figure 5.

230 As shown in the figure of q - h_{max}, the difference of h_{max} between promenade width 0 m and 20
 231 m is significant: to up ~100 l/s/m the ratio is almost 2. Looking at the figure of q - u_{max}, the difference
 232 of the maximum velocity is not significant unless the highest overtopping discharges around ~100
 233 l/s/m.



234
235

Figure 4. Comparison between promenade width 0 m and 20 m on q-Vmax (Average overtopping discharge - maximum individual overtopping volume)



236
237

Figure 5. Comparison between promenade width 0 m and 20 m on q-hmax (upper figure) and q-umax (lower figure).

238 3.2.3. Time evolution of overtopping flow characteristics

239 It is interesting that on one hand the $q-V_{\max}$ gives very similar relationship between different
 240 promenade widths and on the other hand $q-h_{\max}$ shows a strong influence of the promenade width.
 241 In order to understand these differences, the time series of flow properties (time dependent
 242 overtopping flow depth h , velocity u and acceleration) under an overtopping event of similar V (both
 243 case around 1000 l/m, see Table 2) is visualized in Figure 6. Note that the V in this specific example is
 244 not V_{\max} (maximum overtopping volume) in each case. In addition to u and h , the drag and inertia
 245 force acting on a person standing on the promenade is also calculated using the Morison equation
 246 since time evolution of the forces will be more relevant to the stability of a person standing on a
 247 promenade. In this case, two times of a cylinder with the diameter of 0.1 m are used to representing
 248 a person with two legs. Due to the nature of the equation, importance of u is higher than h (cfr. F is
 249 proportional to u^2 and h). As can be seen the drag force is dominant and the inertia force is somewhat
 250 smaller in this case.

251 From Figure 6, it is obvious that the h of the case with promenade length 0 m gives a higher peak
 252 while the flow duration is significantly different. The overtopping of the case with promenade width
 253 20 m lasts about 4 times longer than one in promenade 0 m and this is how it gives the similar V . The
 254 overtopping flow depth of the overtopping waves are decreasing due to the gravity acting on the
 255 overtopped bore when it is propagating over the promenade. These relationships indicate that the
 256 overtopping flow depth and flow velocity will be more relevant to describe the overtopping hazard
 257 compared to the individual overtopping volume V , in the case of gentle and shallow foreshore.

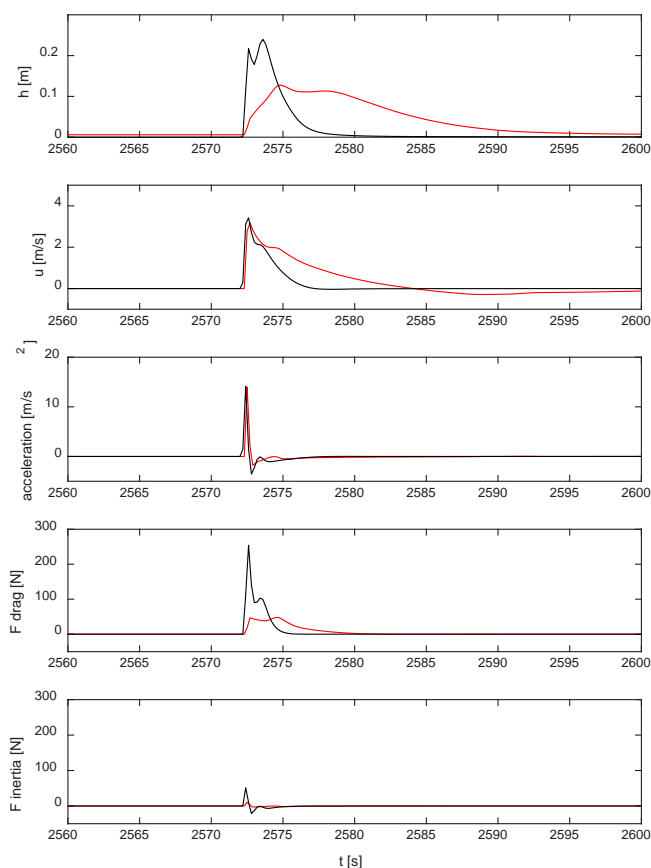
258 Risk on pedestrians on the promenade is often evaluated by the overtopping flow depth and
 259 flow velocity [3–5]. Those are relevant parameters for the stability of a person exposed to the flows:
 260 the higher flow depth and flow velocity the lower the stability of a person. However, looking at
 261 Figure 6, one can see that the timing of the maximum layer thickness and layer velocity of the selected
 262 time window is different. It indicates that only the combination of the maximum values do not
 263 describe the hazard properly.

264

Table 2. Variation of test parameters and the values

Case [-]	Promenade length [m]	V [l/m]
RSK_7_5_12_69_00_00	0	1043
RSK_7_5_12_65_95_20	20	1109

265

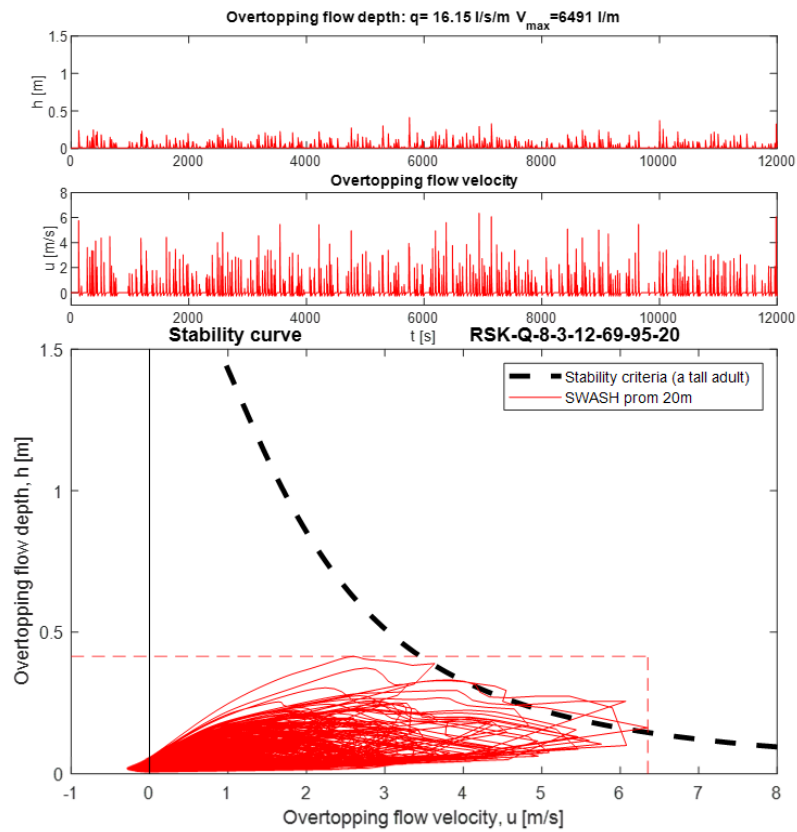


266 **Figure 6.** Time series of h , u , acceleration, F_{drag} and $F_{inertia}$ for the case which V is around 1000
 267 l/m.

268 3.2.4. Overtopping flow characteristics and stability

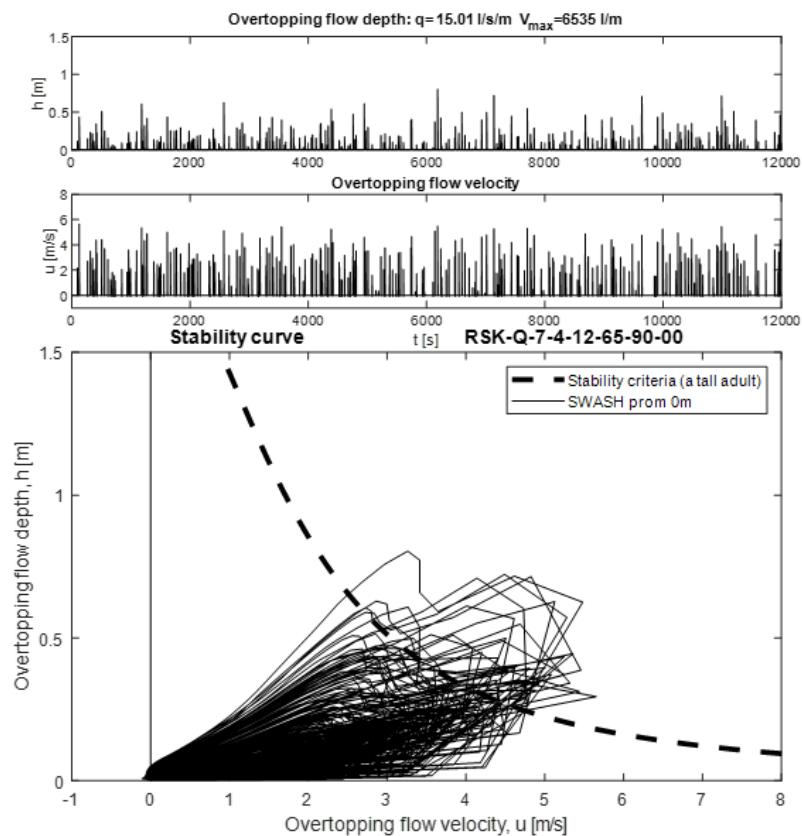
269 Stability is one of the key factors for the safety of the people. Endoh and Takahashi discussed
 270 the human stability taking into account different human instability mode, slipping and tumbling.
 271 Sandoval and Bruce [4] revisited it taking into account the buoyancy and its position, and shows
 272 different criteria by ages and genders. The dashed line shown in Figure 7 is criteria for a tall adult,
 273 the highest criteria. The criteria is expressed as a line by the combination of u and h . However, as
 274 explained earlier, in general u_{max} and h_{max} do not occur at the exactly same moment (there is a time-
 275 lag). If one want to check stability properly, then one needs to use a model which can describe the
 276 combination of u and h in a time series. The red line shows the time series of the u and h obtained at
 277 the end of the 20 m promenade from the SWASH model. Since it is based on 1000 waves, the line goes
 278 the same trajectory many times. The case shown in the figure is 16.2 l/s/m with $V_{max}=6491$ l/m and the
 279 highest part the of the time dependent u - h line is located at the edge of the stability curve. In case the
 280 stability is evaluated by stand-alone h_{max} (horizontal red dotted line) in combination with stand-alone
 281 u_{max} (vertical red dotted line), then the hazard is overestimated as can be seen in the figure.

282 Figure 8 shows a case with very similar q and V_{max} ($q=15.0$ l/s/m and $V_{max}=6535$ l/m) but the
 283 promenade width is 0 m. In this case the h - u line exceeds the stability curve clearly and thus the risk
 284 is higher. It is the same observation as described in the last section 3.2.3: the overtopping hazard is
 285 not always a function of the overtopping discharge nor maximum individual overtopping volume
 286 but on the u and h (in the gentle and shallow foreshore case at least).



287 **Figure 7.** Time series of h and u (the first and second figures) and h - u relationship calculated in
 288 SWASH versus stability curve of a tall adult (the third figure): RSK_Q_8_3_12_69_95_20 00 (a case in
 289 which V is around 6500 l/s/m, and the promenade width of 0 m).

290

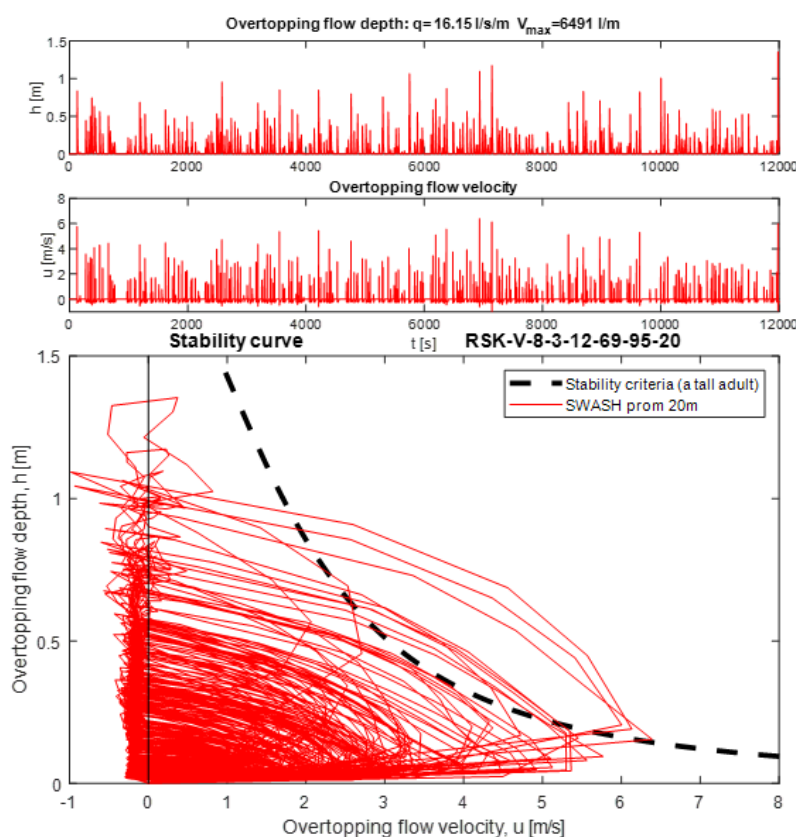


291 **Figure 8.** Time series of h and u (the first and second figures) and h - u relationship calculated in
 292 SWASH versus stability curve of a tall adult (the third figure): RSK_Q_7_4_12_65_90_00 (a case in
 293 which V is around 6500 l/s/m, and the promenade width of 0 m).

294 3.3. Overtopping flow properties in front of a vertical wall

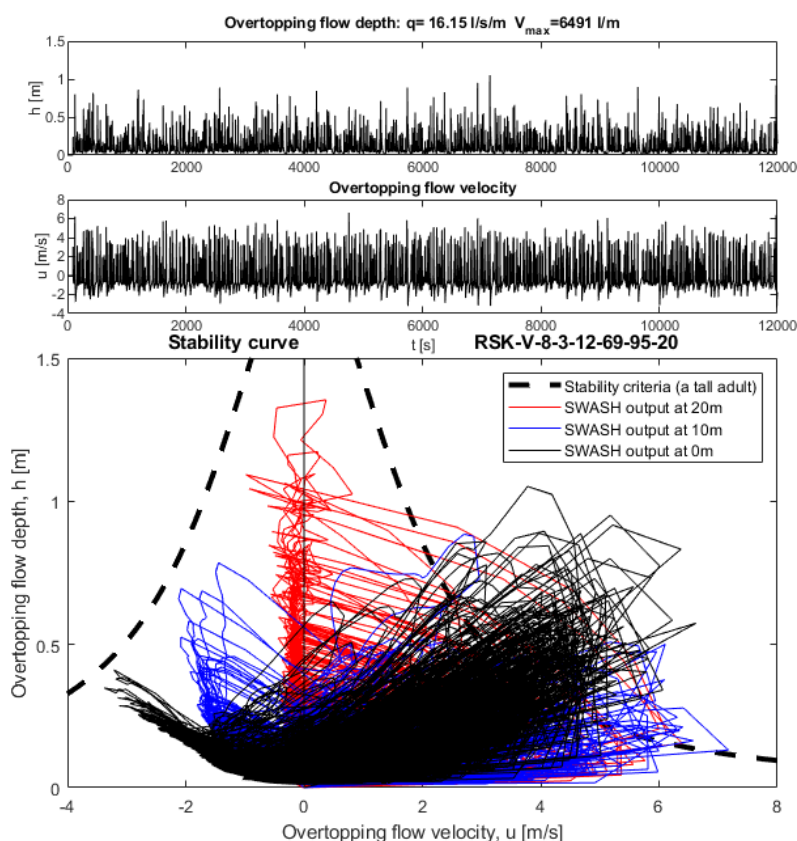
295 In case there is a vertical wall at the end of the promenade, waves are reflected at the wall and
 296 go back to the sea. Figure 9 shows the h - u time series of the same wave case in Figure 7 but with a
 297 vertical wall at the end of the promenade. Note that the h - u output point is just in front of the vertical
 298 wall. As can be seen in the figure, the water level (i.e. h) in front of the wall becomes very high due
 299 to the reflection. The height becomes more than two times of the one in the case without a vertical
 300 wall. Actually, the incident waves are not any more the shape of the wave but a bore, and thus the
 301 wave height can exceed two times of the incident wave height (cfr. standing wave). Especially at the
 302 end of the promenade, the duration of the bore becomes much longer (e.g. four times longer than one
 303 in the case of promenade width 0 m) as explained in section 3.2.2. Thus the flow of the long bore locks
 304 up the water mass in front of the vertical wall and eventually the water level becomes much higher
 305 (the highest level $h \sim 1.3$ m) than the incident bore height (the highest level $h \sim 0.5$ m). During this
 306 process, the h - u line exceeds the stability curve significantly. It is an example of extra possible risk in
 307 the overtopping on the promenade: a structure can increase the hazard. When it reached to the
 308 highest water level, the velocity becomes around zero, and then the reflected waves go back to the
 309 sea as if it is a dam break flow.

310 Figure 10 shows the two extra time series of h - u . The blue line shows h - u at the middle of the
 311 promenade and the black line shows h - u at the beginning of the promenade. These lines exceeded
 312 the stability curve for the incident bore since these are located more seaside. However extra attention
 313 is necessary at the h - u line for the return flow (i.e. line where $u < 0$ m/s). The negative velocity at
 314 the middle of the promenade exceeds 2 m/s and one at the beginning of the promenade exceeds 3 m/s
 315 in this case. Even though the return flow does not reached to the mirrored stability curve, but the values
 316 are not small: a person already fallen down due to the incident bore can be pulled into the sea by the
 317 return flow.



318
319
320
321

Figure 9. Time series of h and u (the first and second figures) and h - u relationship calculated in SWASH versus the stability curve of a tall adult (the third figure): RSK_W_8_3_12_69_95_20 (a vertical wall case corresponding to the case in which V is around 6500 l/s/m, and the promenade width of 20 m).



322
323
324
325

Figure 10. Time series of h and u (the first and second figures) and h - u relationship calculated in SWASH versus the stability curve of a tall adult (the third figure) at 3 output points: RSK_W_8_3_12_69_95_20 (a vertical wall case corresponding to the case in which V is around 6500 l/s/m, and the promenade width of 20 m).

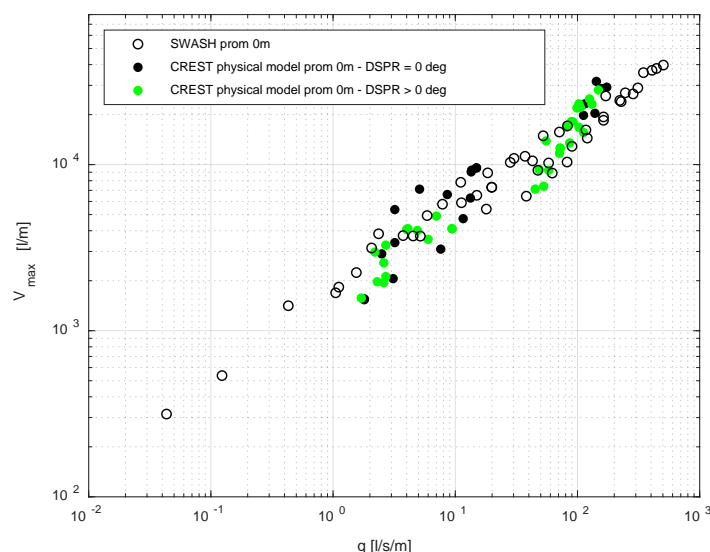
326 4. Discussion

327 4.1. On accuracy of the model

328 In this study, the validated model is used to derive u and h . The accuracy of the model in terms
329 of wave transformation and run-up on the dike is confirmed in [16,32]. Looking into [16], the
330 overtopping estimation has a certain scatter especially when q is small. However further validation
331 confirmed using the data of CREST, the relationship between q and V_{max} , which shows an excellent
332 match to the physical model test data. Note that the accuracy of h and u in time domain has not been
333 confirmed yet in the present study.

334 The modelling is conducted in 2DV and thus the directional spreading effect is not included.
335 The wave propagation and interaction process with the reflected waves in 3D is different from in
336 2DV as shown in [30]. The directional spreading effect is twofold – one is wave transformation from
337 offshore to the toe, and the other one is from the toe to the end of the dike slope where overtopping
338 is measured [6]. In this study mean overtopping discharge q and maximum individual volume V_{max}
339 are compared for promenade 0 m and 20 m cases. However, the influence of the directional spreading
340 is expected to be limited because the relation between q and V_{max} is similar. The green points depicted
341 in Figure 11 show the q - V_{max} relationship from the CREST physical model where directional
342 spreading is greater than 0 degree (i.e. 12, 16, 20 and 31.5 degree). As can be seen, the green points
343 are shown in the could of the black points (i.e. directional spreading is zero) while the majority of the

344 green points are located in the lower part of the entire cloud. Strictly speaking directional spreading
 345 effect on q - V can be different for the case of 20 m promenade since the oblique wave can make the
 346 overtopping trajectory longer than one of perpendicular attack, namely the effective promenade
 347 width will be longer. When the length of the promenade width is longer, the V can be slightly smaller.



348 **Figure 11.** Comparison between DSPR=0 and DSPR>0 of physical models on q - V_{max} (Average
 349 overtopping discharge - maximum individual overtopping volume) for the case of promenade width
 350 0 m

351 *4.2. On the overtopping parameters*

352 Needless to say that q and V_{max} is still very important parameters to have the first idea to estimate
 353 how severe will be the overtopping event. However time dependent value u and h are more relevant
 354 to understand the risk on the dike in details as shown in this study. These parameters have a direct
 355 link to the stability of a person. On top of these parameters, acceleration (a) and overtopping event
 356 duration (t_o) can be also parameters to give extra information to characterize the overtopping flow on
 357 a dike: acceleration in combination with h can give extra forcing of inertia and duration is also a
 358 useful parameter to understand how the overtopping is distributed in time.

359 *4.3. On the risk*

360 Oppenheimer et al. [33] identified 6 sea level rise (SLR) scenarios. Some of them indicated to
 361 have structures in front of the properties to defend from the SLR. From the present study, it became
 362 clear that the time dependent h and u needs to be evaluated on top of average overtopping discharge
 363 and V_{max} , in order to understand the risk. Apparently the influence of the promenade is positive in a
 364 sense that it reduces not only q but also h , as also indicated in [6]. Eventually the forcing on
 365 pedestrians, vehicles and structures will be reduced due to the effect of the promenade. The effect
 366 can be strengthened if extra obstacles are placed on top of the promenade, for instance sea walls and
 367 vegetation. The key will be how to reduce q and V_{max} and also make overtopping event duration (t_o)
 368 longer, so that h - u line stays in a small range.

369 The forcing on the structure is governed by the hydrodynamics [34]. In this study, the façade is
 370 assumed to be broken. However if the façade is strong enough the safety of the people inside the
 371 building is maintained. According to Streicher [35], the force acting on a vertical wall on the
 372 promenade can be the quasi-hydrostatic in gentle and shallow foreshore case. Therefore, the force in
 373 such case can be estimated roughly if h_{max} is known. One of the effective evacuation strategies is the
 374 vertical evacuation, however in order to make sure this evacuation method is safe, first the stability
 375 of the building needs to be guaranteed. That is the reason why estimation of force acting on a building
 376 is necessary. [32] indicated that SWASH is also capable to estimate F on a vertical structure, but it is

377 not explored in this study. In case detailed hydrodynamics needs to be obtained for complex
378 structures, detailed hydrodynamic modelling (e.g. [22,24]) will be an alternative.

379 5. Conclusions

380 In this study overtopping risk on a dike in gentle and shallow foreshores are investigated using
381 SWASH, a NLSW equation solver. The model has been validated in different studies applied for
382 shallow foreshores but it is further validated in terms of maximum individual volume based on a
383 physical model. One of the benefits to use SWASH in this study is that the model can output h and u
384 in time series while measurement of u on a dike in physical model test is often a challenge. Using
385 SWASH the risk on the dike can be evaluated in details, in function of time. On top, SWASH is
386 relatively a light wave model, and thus it is possible to obtain overtopping flows in different wave
387 conditions and bathymetries: in this study total ~200 cases are simulated.

388 It is often the case in practice that the coastal safety is evaluated by the average overtopping
389 discharge and maximum individual volume V_{\max} . However it becomes clear from this study that
390 overtopping risk is not only characterized by q and V : time dependent h and u are also useful and
391 even better parameters to characterize risks on dikes more in details. For instance, two cases in the
392 example of this study show different h , even though the two cases show very similar q and V_{\max} . This
393 was due to the influence of the promenade which made h smaller and the duration longer. It is noted
394 that the combination of stand-alone h_{\max} and u_{\max} can lead an overestimation of the hazard and
395 therefore time dependent h and u are better for the proper assessment.

396 In addition to the overtopping flow on plain dikes, the influence of a vertical wall at the end of
397 the promenade is also evaluated in this study. The results show that the vertical wall can influence
398 on the people's safety on the promenade in a negative way. The bore can create a higher flow depth
399 compared to the case without a vertical wall and it becomes an extra risk o . Depending on the position
400 on the promenade, a relatively high negative velocity was also observed in the simulation.

401 Further study on the characterization of overtopping waves will be useful since a proper
402 assessment of wave overtopping is an essential key for designing coastal structures which provides
403 safety for people in coastal area. Numerical modelling is a strong tool to evaluate risks in different
404 scenarios.

405 **Author Contributions:** Conceptualization, T.S.; methodology, T.S., C.A., T.Y.; analysis, T.S.; investigation, T.S.;
406 writing—original draft preparation, T.S.; writing—review and editing, C.A., T.Y, T.V.; visualization, T.S.;
407 supervision, T.V.; project administration, T.V. All authors have read and agreed to the published version of the
408 manuscript.

409 **Funding:** This research was part of the CREST (Climate REsilient CoaST) project
410 (<http://www.crestproject.be/en>), funded by the Flemish Agency for Innovation by Science and Technology, grant
411 number 150028. Corrado Altomare acknowledges funding from the European Union's Horizon 2020 research
412 and innovation programme under the Marie Skłodowska-Curie grant agreement No.:792370.

413 **Acknowledgments:** In this section you can acknowledge any support given which is not covered by the author
414 contribution or funding sections. This may include administrative and technical support, or donations in kind
415 (e.g., materials used for experiments).

416 **Conflicts of Interest:** The authors declare no conflict of interest. The funders had no role in the design of the
417 study; in the collection, analyses, or interpretation of data; in the writing of the manuscript, or in the decision to
418 publish the results.

419 References

- 420 1 Weisse, R.; von Storch, H.; Niemeier, H. D.; Knaack, H. Changing North Sea Storm Surge Climate: An
421 Increasing Hazard? *Ocean Coast. Manag.* **2012**, *68*, 58–68. <https://doi.org/10.1016/j.ocecoaman.2011.09.005>.
- 422 2 Neumann, B.; Vafeidis, A. T.; Zimmermann, J.; Nicholls, R. J. Future Coastal Population Growth and
423 Exposure to Sea-Level Rise and Coastal Flooding - A Global Assessment. *PLoS One* **2015**, *10* (3).
424 <https://doi.org/10.1371/journal.pone.0118571>.

- 425 3 Endoh, K.; Takahashi, S. Numerically Modeling Personnel Danger on a Promenade Breakwater Due to
426 Overtopping Waves. In *24th International Conference on Coastal Engineering, October 23-28, 1994, Kobe,*
427 *Japan*; 1995; pp 1016–1029.
- 428 4 Bruce, T.; Sandoval, C. Wave Overtopping Hazard to Pedestrians: Video Evidence from Real Accidents.
429 In *Coasts, Marine Structures and Breakwaters 2017*; 2017; pp 501–512.
- 430 5 Allsop, N. W. H.; Bruce, T.; Pullen, T.; van der Meer, J. Direct Hazards From Wave Overtopping – the
431 Forgotten Aspect of Coastal Flood Risk Assessment? *43rd DEFRA Flood Coast. Manag. Conf.* **2008**, No.
432 July, 1–11.
- 433 6 Altomare, C.; Gironella, X.; Suzuki, T.; Viccione, G.; Saponieri, A. Overtopping Metrics and Coastal
434 Safety: A Case of Study from the Catalan Coast. *J. Mar. Sci. Eng.* **2020**, *8* (8).
435 <https://doi.org/10.3390/JMSE8080556>.
- 436 7 Arrighi, C.; Oumeraci, H.; Castelli, F. Hydrodynamics of Pedestrians' Instability in Floodwaters. *Hydrol.*
437 *Earth Syst. Sci.* **2017**, *21* (1), 515–531. <https://doi.org/10.5194/hess-21-515-2017>.
- 438 8 Arrighi, C.; Pregnolato, M.; Dawson, R. J.; Castelli, F. Preparedness against Mobility Disruption by
439 Floods. *Sci. Total Environ.* **2019**, *654*, 1010–1022. <https://doi.org/10.1016/j.scitotenv.2018.11.191>.
- 440 9 Schüttrumpf, H.; Oumeraci, H. Scale and Model Effects in Crest Level Design. In *2nd Coastal Symposium,*
441 *Höfn, Iceland, 5–8 June 2005*; 2005; pp 1–12.
- 442 10 Nørgaard, J. Q. H.; Lykke Andersen, T.; Burcharth, H. F.; Steendam, G. J. Analysis of Overtopping Flow
443 on Sea Dikes in Oblique and Short-Crested Waves. *Coast. Eng.* **2013**, *76*, 43–54.
444 <https://doi.org/10.1016/j.coastaleng.2013.01.012>.
- 445 11 Mares-Nasarre, P.; Argente, G.; Gómez-Martín, M. E.; Medina, J. R. Overtopping Layer Thickness and
446 Overtopping Flow Velocity on Mound Breakwaters. *Coast. Eng.* **2019**, *154* (September).
447 <https://doi.org/10.1016/j.coastaleng.2019.103561>.
- 448 12 van Bergeijk, V. M.; Warmink, J. J.; van Gent, M. R. A.; Hulscher, S. J. M. H. An Analytical Model of
449 Wave Overtopping Flow Velocities on Dike Crests and Landward Slopes. *Coast. Eng.* **2019**, *149* (October
450 2018), 28–38. <https://doi.org/10.1016/j.coastaleng.2019.03.001>.
- 451 13 Chen, X.; Jonkman, S. N.; Pasterkamp, S.; Suzuki, T.; Altomare, C. Vulnerability of Buildings on Coastal
452 Dikes Due to Wave Overtopping. *Water (Switzerland)* **2017**, *9* (6). <https://doi.org/10.3390/w9060394>.
- 453 14 Allsop, N. W. H.; Bruce, T. ; De Rouck, J. ; Kortenhuis, A. ; Pullen, T. ; Schüttrumpf, H. ; Troch, P. ;
454 van der Meer, J.W.; Zannutigh, B. *Manual on Wave Overtopping of Sea Defences and Related Structures. An*
455 *Overtopping Manual Largely Based on European Research, but for Worldwide Application*, 2nd ed.; 2018.
- 456 15 Altomare, C.; Suzuki, T.; Chen, X.; Verwaest, T.; Kortenhuis, A. Wave Overtopping of Sea Dikes with
457 Very Shallow Foreshores. *Coast. Eng.* **2016**, *116*, 236–257. <https://doi.org/10.1016/j.coastaleng.2016.07.002>.
- 458 16 Suzuki, T.; Altomare, C.; Veale, W.; Verwaest, T.; Trouw, K.; Troch, P.; Zijlema, M. Efficient and Robust
459 Wave Overtopping Estimation for Impermeable Coastal Structures in Shallow Foreshores Using
460 SWASH. *Coast. Eng.* **2017**, *122*. <https://doi.org/10.1016/j.coastaleng.2017.01.009>.
- 461 17 Lashley, C. H.; Bricker, J. D.; Bricker, J. D.; Van Der Meer, J.; Van Der Meer, J.; Altomare, C.; Altomare,
462 C.; Suzuki, T.; Suzuki, T. Relative Magnitude of Infragravity Waves at Coastal Dikes with Shallow
463 Foreshores: A Prediction Tool. *J. Waterw. Port, Coast. Ocean Eng.* **2020**, *146* (5), 1–17.
464 [https://doi.org/10.1061/\(ASCE\)WW.1943-5460.0000576](https://doi.org/10.1061/(ASCE)WW.1943-5460.0000576).
- 465 18 Zijlema, M.; Stelling, G.; Smit, P. SWASH : An Operational Public Domain Code for Simulating Wave Fi
466 Elds and Rapidly Varied Fl Ows in Coastal Waters. *Coast. Eng.* **2011**, *58* (10), 992–1012.
467 <https://doi.org/10.1016/j.coastaleng.2011.05.015>.

- 468 19 Smit, P.; Zijlema, M.; Stelling, G. Depth-Induced Wave Breaking in a Non-Hydrostatic, near-Shore Wave
469 Model. *Coast. Eng.* **2013**, *76*, 1–16. <https://doi.org/10.1016/j.coastaleng.2013.01.008>.
- 470 20 Rijnsdorp, D. P.; Zijlema, M. Simulating Waves and Their Interactions with a Restrained Ship Using a
471 Non-Hydrostatic Wave-Flow Model. *Coast. Eng.* **2016**, *114*, 119–136.
472 <https://doi.org/10.1016/j.coastaleng.2016.04.018>.
- 473 21 Suzuki, T.; Hu, Z.; Kumada, K.; Phan, L. K.; Zijlema, M. Non-Hydrostatic Modeling of Drag, Inertia and
474 Porous Effects in Wave Propagation over Dense Vegetation Fields. *Coast. Eng.* **2019**, *149* (135), 49–64.
475 <https://doi.org/10.1016/j.coastaleng.2019.03.011>.
- 476 22 Gruwez, V.; Altomare, C.; Suzuki, T.; Streicher, M.; Cappietti, L.; Kortenhuis, A.; Troch, P. Validation of
477 RANS Modelling for Wave Interactions with Sea Dikes on Shallow Foreshores Using a Large-Scale
478 Experimental Dataset. *J. Mar. Sci. Eng.* **2020**, *8* (9), 650. <https://doi.org/10.3390/jmse8090650>.
- 479 23 Crespo, A. J. C.; Domínguez, J. M.; Rogers, B. D.; Gómez-Gesteira, M.; Longshaw, S.; Canelas, R.;
480 Vacondio, R.; Barreiro, A.; García-Feal, O. DualSPHysics: Open-Source Parallel CFD Solver Based on
481 Smoothed Particle Hydrodynamics (SPH). *Comput. Phys. Commun.* **2015**, *187*, 204–216.
482 <https://doi.org/10.1016/j.cpc.2014.10.004>.
- 483 24 Altomare, C.; Crespo, A. J. C.; Domínguez, J. M.; Gómez-Gesteira, M.; Suzuki, T.; Verwaest, T.
484 Applicability of Smoothed Particle Hydrodynamics for Estimation of Sea Wave Impact on Coastal
485 Structures. *Coast. Eng.* **2015**, *96*, 1–12. <https://doi.org/10.1016/j.coastaleng.2014.11.001>.
- 486 25 Altomare, C.; Domínguez, J. M.; Crespo, A. J. C.; Suzuki, T.; Caceres, I.; Gómez-Gesteira, M.
487 Hybridization of the Wave Propagation Model SWASH and the Meshfree Particle Method SPH for Real
488 Coastal Applications. *Coast. Eng. J.* **2016**. <https://doi.org/10.1142/S0578563415500242>.
- 489 26 Vandebeek, I.; Gruwez, V.; Altomare, C.; Suzuki, T.; Vanneste, D.; Roo, S. D.; Toorman, E.; Troch, P.
490 Towards an Efficient and Highly Accurate Coupled Numerical Modelling Approach for Wave
491 Interactions with a Dike on a Very Shallow Foreshore. In *Coastlab 2018*; 2018.
- 492 27 Suzuki, T.; De Roo, S.; Altomare, C.; Zhao, G.; Kolokythas, G. K.; Willems, M.; Verwaest, T.; Mostaert, F.
493 *Toetsing Kustveiligheid 2015 - Methodologie: Toetsingsmethodologie Voor Dijken En Duinen*, 10.0.; WL
494 Rapporten; Waterbouwkundig Laboratorium: Antwerpen, 2016; Vol. 14_014.
- 495 28 Rijnsdorp, D. P.; Smit, P. B.; Zijlema, M. Non-Hydrostatic Modelling of Infragravity Waves under
496 Laboratory Conditions. *Coast. Eng.* **2014**, *85*, 30–42. <https://doi.org/10.1016/j.coastaleng.2013.11.011>.
- 497 29 Vasarmidis, P.; Stratigaki, V.; Suzuki, T.; Zijlema, M.; Troch, P. Internal Wave Generation in a Non-
498 Hydrostatic Wave Model. *Water (Switzerland)* **2019**, *11* (5). <https://doi.org/10.3390/w11050986>.
- 499 30 Altomare, C.; Suzuki, T.; Verwaest, T. Influence of Directional Spreading on Wave Overtopping of Sea
500 Dikes with Gentle and Shallow Foreshores. *Coast. Eng.* **2020**, *157* (May 2019), 103654.
501 <https://doi.org/10.1016/j.coastaleng.2020.103654>.
- 502 31 Tortora, S. Statistical Characterisation of Overtopping Volumes for Sea Dikes in Very Shallow Foreshore
503 Condition under Short- and Long-Crested Waves Action, 2018.
- 504 32 Suzuki, T.; Altomare, C.; De Roo, S.; Vanneste, D.; Mostaert, F. *Manning's Roughness Coefficient in*
505 *SWASH: Application to Overtopping Calculation*, Version 2.; FHR reports; Flanders Hydraulics Research:
506 Antwerp, 2018; Vol. 17_026_1.
- 507 33 Oppenheimer, M., B.C. Glavovic, J. Hinkel, R. van de Wal, A.K. Magnan, A. Abd-Elgawad, R. Cai, M.
508 Cifuentes-Jara, R.M. DeConto, T. Ghosh, J. Hay, F. Isla, B. Marzeion, B. Meyssignac, and Z. S. Sea Level
509 Rise and Implications for Low-Lying Islands, Coasts and Communities. In *IPCC Special Report on the*
510 *Ocean and Cryosphere in a Changing Climate*; 2019.

- 511 34 Chen, X.; Hofland, B.; Altomare, C.; Suzuki, T.; Uijttewaal, W. Forces on a Vertical Wall on a Dike Crest
512 Due to Overtopping Flow. *Coast. Eng.* **2015**, *95*, 94–104. <https://doi.org/10.1016/j.coastaleng.2014.10.002>.
- 513 35 Streicher, M.; Kortenhaus, A.; Marinov, K.; Hirt, M.; Hughes, S.; Hofland, B.; Scheres, B.; Schüttrumpf,
514 H. Classification of Bore Patterns Induced by Storm Waves Overtopping a Dike Crest and Their Impact
515 Types on Dike Mounted Vertical Walls - A Large-Scale Model Study. *Coast. Eng. J.* **2019**, *61* (3), 321–339.
516 <https://doi.org/10.1080/21664250.2019.1589635>.
- 517



© 2020 by the authors. Submitted for possible open access publication under the terms and conditions of the Creative Commons Attribution (CC BY) license (<http://creativecommons.org/licenses/by/4.0/>).

518